Detection of Urinary Albumin Using a Novel "Turn-on" Fluorescent Probe with Aggregation-Induced Emission Characteristics

Qi Hu,[#[a]] Bicheng Yao,[#[b]] Tze Cin Owyong,[[b, c]] Sharon Prashanth,[[a]] Changyu Wang,[[a]] Xinyi Zhang,[[a, d]] Wallace W. H. Wong,[[c]] Youhong Tang,*[[a, d]] and Yuning Hong*[[b]]

[a] Q. Hu, S. Prashanth, C. Wang, X. Zhang, Prof. Dr. Y. Tang
Medical Device Research Institute, College of Science and Engineering,
Flinders University
South Australia 5042, Australia
E-mail: youhong.tang@flinders.edu.au

[b] Dr. B. Yao, T. C. Owyong, Dr. Y. Hong
Department of Chemistry and Physics, La Trobe Institute for Molecular Science,
La Trobe University
Victoria, 3086 Australia
E-mail: y.hong@latrobe.edu.au

[c] T. C. Owyong, Dr. W. W. H. Wong
ARC Centre of Excellence in Exciton Science, School of Chemistry,
Bio21 Institute,
The University of Melbourne
Victoria, 3010 Australia

[d] X. Zhang, Prof. Dr. Y. Tang
Australia-China Joint Research Centre for Personal Health Technologies,
Flinders University
South Australia 5042, Australia

# These authors contribute equally.

Supporting information for this article is given via a link at the end of the document.

Abstract: Human serum albumin (HSA) is a broadly used biomarker for the diagnosis of various diseases such as chronic kidney disease. Here, a fluorescent probe **TC426** with aggregation-induced emission (AIE) characteristics is reported as a sensitive and specific probe for HSA. This probe is non-emissive in aqueous solution, meanwhile it shows bright fluorescence upon interacting with HSA, which makes it applicable in detecting HSA with a high signal to noise ratio. Besides, the fluorescence of **TC426** exhibits a high linear correlation with the concentration of albumin in the range of microalbumin (20-200 mg/L), which has a significant importance for the early diagnosis of glomerulus related diseases. Compared with previously reported HSA probes **TPE-4TA** and **BSPOTPE**, **TC426** shows comparable anti-interference ability towards creatinine and other major components in urine but is excited by a longer excitation wavelength at the visible light range. Finally, with the established assay, **TC426** shows excellent performance in detecting HSA in real human urine, indicating its great potential in practical urinalysis.

Introduction

Human serum albumin (HSA) is the most abundant protein in human blood plasma, accounting for 55–60% of the measured serum proteins.[1] As the major soluble protein component in human serum, it has many physiological functions. For example, HSA maintains 80% of normal plasma colloidal osmotic activity. Besides, due to the existence of Gibbs-Donnan effect, it provides an attractive force for the retention of positively charged solutes in blood vessels.[1-2] Thanks to the existence of abundant reduced sulfhydryl groups, HSA also has good free radical scavenging ability.[3] In terms of the structure of HSA, it is composed of three α-helical domains I, II and III, with each one contains two subdomains A and B.[2b] Due to the different helical structures, the subdomains show different ligand binding affinity, endowing HSA with good binding capability towards various endogenous and exogenous ligands. As a result, HSA can bind with many substances including bilirubin, vitamin D, thyroxin, etc., and adjust their biologic activity, distribution, and rate of clearance.[4]

Since certain diseases may alter the distribution of albumin between the intravascular and extravascular compartments [1], detecting HSA level in biological fluids is clinically used for the diagnosis of many diseases, such as cancer, diabetes, liver disease, inflammation, rheumatic disease, cardiovascular diseases, etc.[5] For example, urinary albumin is deemed as an important clinical indicator of chronic kidney disease (CKD). For healthy people, very little albumin leaks through glomerulus into the urine, with a urinary albumin level less than 30 mg/L. However, in end-stage kidney failure (the last stage of CKD), a large amount of albumin will be spilled into the urine, resulting in a urinary albumin concentration greater than 300 mg/L. At present, the routine methods used to detect urinary albumin are immunoassay and colorimetry-based assays.[6] The detection limit for immunoassay is 2-10 mg/L, with a tendency to underestimate the amount of albumin due to the chemical structure of albumin and complexity of urine environment. Hence, the immunoassay is deemed as an inaccurate method for testing microalbumin.[7] Moreover, there are a variety of colorimetric methods, including the Lowry assay, Biuret and Bradford test.[8] These methods, however, have low detection accuracy and do not selectively respond to HSA. A practical application of colorimetry is urine dipsticks, that have low detection sensitivity with a detection limit greater than 150 mg/L.[9]

Fluorescence based strategies have attracted increasing attention from the biosensing field, due to the advantages of simple operation, rapid response, high sensitivity, and cost efficiency. Among various fluorescent probes, the aggregation induced emission (AIE)-based ones demonstrated outstanding performances, such as application to a broad concentration range, good photostability, low background noise, large Stokes shifts, etc.[10] As such, AIE-based techniques may be a good substitution for current test methods for HSA. In 2010, Tang and coworkers first reported an AIE probe, a tetraphenylethylene (TPE)

derivative **BSPOTPE** for quantitative detection of HSA.[11] This probe is non-fluorescent in PBS buffer, but becomes emissive in the presence of HSA. The established fluorescent method exhibited a broad linear dynamic range (LDR) of 0-6.76 mg/L, a detection limit (LOD) as low as 0.0676 mg/L, and an excellent selectivity to HSA. Additionally, the sensing process was also demonstrated in artificial urine, showing great potential in real-life application. After this work, many AIE probes have been developed for HSA detection and quantification.[12] Recently, Tu et al. reported another TPE derivative, **TPE-4TA**, for specific and quantitative detection of HSA.[13] In this work, tetrazolate, which has a strong binding affinity toward HSA, was used as the targeting moiety. The HSA sensing performance was first evaluated in PBS buffer, showing a LOD down to 14.2 μg/L and a good LDR of 0.02-2500 mg/L. The feasibility of this probe for urinary albumin detection was further validated in clinical urine samples. All these results indicated that **TPE-4TA** is superior in HSA detection than other AIE-active HSA probes. However, the synthesis of **TPE-4TA** requires harsh conditions and highly toxic cuprous cyanide. Thus, the difficulty in synthesis may limit its further application.

In this work, we designed a novel fluorescent dye **TC426** which can be synthesized through a simple two-step synthetic route. This probe is non-fluorescent when molecularly dissolved in aqueous solution but shows strong emission upon aggregation or in a viscous medium, characteristic of typical AIE active molecules. Due to the unique chemical structure and photophysical property, **TC426** can be applied in the detection of HSA, showing comparable results as previously reported HSA probes. To apply probe **TC426** to albumin detection in real urine samples, we evaluated the influence of pH and interfering substances present in urine and demonstrated excellent stability and good selectivity towards HSA. Significantly, satisfactory recovery rates in spiked real human urine samples were obtained by using **TC426** as the fluorescent probe. This indicates that probe **TC426** has great potential in real-world urinary albumin analysis.

Results and Discussion

Probe synthesis and Structural Characterization

The synthetic route to the albumin probe **TC426** is shown in **Scheme 1**. In short, the Knoevenagel condensation reaction between 4-(diethylamino)salicylaldehyde and 1,3-indandione yielded the intermediate compound **2**. Subsequent alkylation of the hydroxy group from compound **2** with 1,3-propanesultone allowed for the introduction of a sodium sulfonate group and formation of the final probe molecule **TC426**. The structure of both compound **2** and **TC426** were characterized by ^{1}H NMR, ^{13}C NMR and HRMS and satisfying results were obtained (**Figure S1**-**S5**).

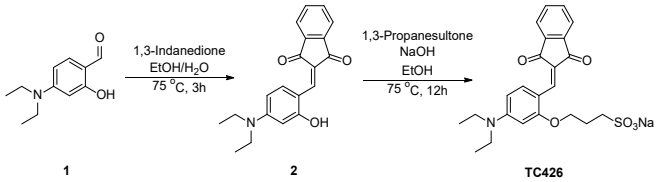

Scheme 1. Synthetic route to probe **TC426**.

Photophysical Property Characterisation

As seen from **Scheme 1,** the conjugation of 1,3-indandione was extended after conjugated with 4-(diethylamino)salicylaldehyde through a carbon-carbon double bond. The presence of the electron acceptor 1,3-indanedione moiety, gives rise to an electron donor-acceptor (D-A) structure in **TC426**. Sodium sulfonate groups further endow **TC426** with good water solubility. We first measured the UV-vis absorbance spectra of **TC426** in different solvents. As shown in **Figure 1A**, minimal differences in spectral character were observed for most of the solvents, with the absorbance maxima wavelength ranging from 494 nm to 512 nm. The spectra measured in toluene was an exception, with a slight blue-shifted absorbance maxima at ~450 nm and a shoulder peak at ~490 nm.

We then examined the fluorescence emission behavior of **TC426** in these solvents (**Figure 1B**). In most cases, when excited under the absorption maxima wavelength, the fluorescence emission spectra of **TC426** does not change significantly, with all the peak wavelengths centred around 535 nm. With regards to the fluorescence emission intensity, some variances can be observed, and minimal emission intensity was recorded in PBS buffer. For the two exceptions measured in chloroform and toluene, new dominant fluorescence maxima were observed at ~655 nm, with only chloroform retaining the previously seen 535 nm peak. A possible explanation for this phenomenon is the formation of large emissive aggregates with red-shifted spectra in the low/non-polar solvents of chloroform and toluene. We then measured the particle sizes of **TC426** in chloroform and toluene using the Dynamic Light Scattering (DLS) technique. The results confirm that large particles of **TC426** with average sizes of 107.2 nm and 175.6 nm were formed in chloroform and toluene respectively (**Figure S6**-**S7**).

Finally, relative fluorescence quantum yields (QYs) of **TC426** in various solvents were measured using fluorescein as the reference. The results summarized in **Table S1** showed the highest QY value of 1.26% in chloroform and lowest QY values of 0.05% in water. Moreover, we plotted the QY value as a function of solvent Lippert-Mataga polarity parameter (**Figure S8**) and found that QY of **TC426** decreases linearly with the increase of solvent polarity. The QYs in toluene, chloroform, DMSO and isopropanol are exceptions, which can be ascribed to the AIE characteristics of **TC426** in poor solvents (toluene and chloroform) or viscous solvents (DMSO and isopropanol). This will be further explained in the next part. In summary, the QY of **TC426** shows typical solvent polarity dependence.

As aforementioned, when molecularly dissolved in PBS buffer, **TC426** is non-emissive under the excitation of 488 nm. However,

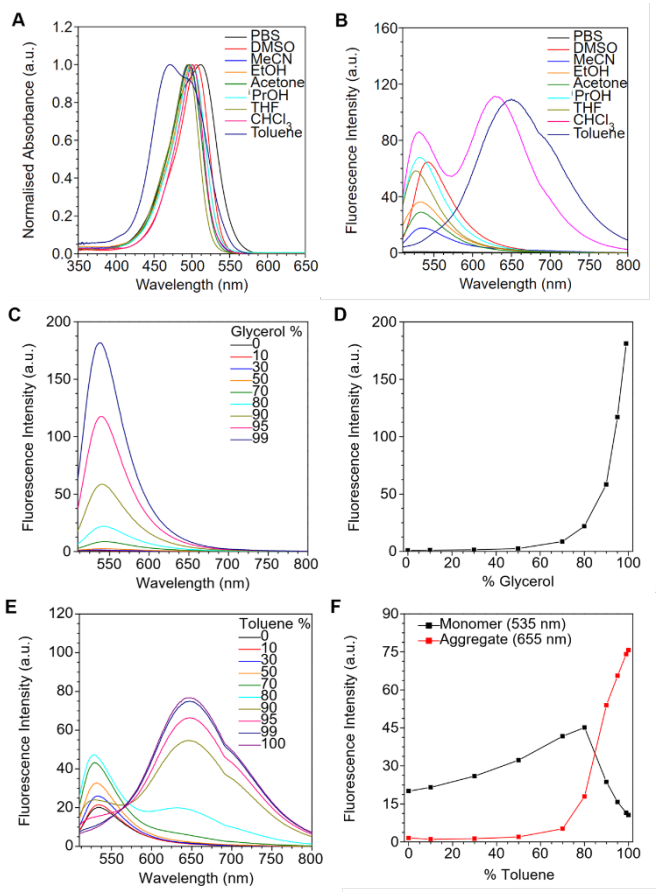

Figure 1. Absorbance and fluorescence emission spectra characterisation for **TC426**. (A) Normalised UV-Vis absorption spectra and (B) Fluorescence emission spectra of **TC426** in different solvents. (C, D) Fluorescence spectra and plot of fluorescence intensity of **TC426** in water/glycerol mixtures, with increasing fraction of glycerol from 0 to 99%. (E, F) Fluorescence spectra and plot of fluorescence intensity of **TC426** in DMSO/toluene mixtures with increasing fraction of toluene from 0 to 100%. Plots were obtained by taking fluorescence emission intensity values at 535 nm and 655nm for monomer and aggregate fluorescence emission, respectively. PBS was Na_2HPO_4 at 20 mM concentration. 10 μM dye concentration and 488 nm excitation wavelength were used for all measurements.

it becomes highly fluorescent when aggregated into large particles or in solid state (**Figure S9**). This feature is completely in conformity with the definition of AIE, which inspired us to further study its AIE behavior. We first measured the fluorescence of **TC426** in water/glycerol mixtures whose viscosity can be increased by adding more glycerol. As shown in **Figure 1C** and **1D**, when the glycerol fraction is above 70 vol%, the fluorescence intensity of probe **TC426** enhances dramatically with the increase of glycerol fractions. This phenomenon can be explained by the rigidification of the molecule structure resulting from the increasing solution viscosity, which blocks the non-radiative decay channels and enhances the fluorescence emission of **TC426**. Fluorescence spectra of **TC426** in DMSO with increasing content of toluene, a poor solvent for **TC426**, were characterized (**Figure 1E** and **1F**). When toluene fraction is below 70 vol%, fluorescence emission spectra peaked at 535 nm were obtained which can be ascribed to the monomeric emission of **TC426**. Affected by the electron D-A structure, the emission of **TC426** monomer was slightly suppressed in polar solvent due to the twisted intramolecular charge transfer (TICT) effect[14], and enhanced when more non-polar solvent was added to weaken the TICT effect. Beyond 70 vol% of toluene, the fluorescence intensity at 535 nm began to decrease significantly, meanwhile a new peak belonging to the aggregates of **TC426** emerged at 655 nm and increased with higher toluene fraction. This result indicates the transition of monomeric to aggregate emission species with the increase of toluene content. The formation of aggregates, instead of quenching fluorescence like traditional aggregation-caused quenching (ACQ) type fluorophores, exhibits fluorescence intensity enhancement, further manifesting the AIE-character of **TC426**.

Quantitative Detection of Human Serum Albumin

Based on our previous research, AIE fluorogens (AIEgens) with periphery-charged groups including sulfonate, carboxylate, trialkyl-ammonium, pyridinium, and tetrazolium groups, may have fluorescence enhancements upon binding with HSA.[5c, 13] These functional groups facilitate AIEgens to dissolve in water, thus exhibiting weak fluorescence. When bound to the hydrophobic cavity of HSA, the RIM effect of AIEgens can occur and thus lead to the fluorescence enhancement effect. Since **TC426** is AIE-active and has an alkyl sulfonate group, it may be applied in the detection of HSA. We first studied the fluorescence response of **TC426** towards HSA in PBS buffer (10 mM, pH = 7.4). The time-dependence of probe fluorescence intensity after adding the 1000 mg/L HSA sample was shown in **Figure S10**. Upon addition of HSA, an intense fluorescence signal at 550 nm can be detected. The fluorescence intensity reached equilibrium quickly and was stable within 60 min, indicating the fast response of probe **TC426** towards HSA. In order to further explore its sensitivity, fluorescence titration of probe **TC426** with various concentrations of HSA in PBS buffer was conducted. As shown in **Figure 2A**, the fluorescence intensity of probe **TC426** at 550 nm increased gradually with the increase of HSA concentration. When HSA concentration reached to 1000 mg/L, the fluorescence intensity at 550 nm was enhanced approximately 450 times. Additionally, an excellent linear correlation between the fluorescence intensity and HSA concentration was observed with R^2 = 0.9954 in the concentration range of 0-1000 mg/L (**Figure 2B**). This linear correlation can be further improved in the microalbuminuria range (20-200 mg/L)[15]. Finally, according to the IUPAC-based method, the limit of detection (LOD) of probe **TC426** was calculated to be as low as 0.253 mg/L (3.74 nM). Both the linear dynamic range (LDR) and LOD of **TC426** are comparable to those of other HSA probes, such as **BSPOTPE** (LOD: 0.0676 mg/L; LDR: 0-6.76 mg/L). In brief, probe **TC426** shows good performance in the quantitative detection of HSA, which may find potential applications in urinalysis for kidney disease prediction.

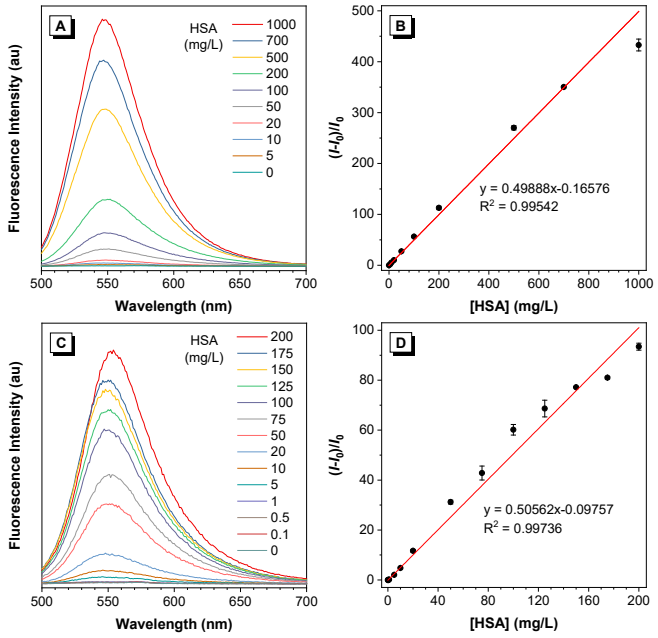

Figure 2. Fluorescence spectra of probe **TC426** in the presence of HSA with concentration ranging from (A) 0-1000 mg/L and (C) 0-200 mg/L. Plot of fluorescence intensity increase fold at 550 nm versus the concentration of HSA ranging from (B) 0-1000 mg/L and (D) 0-200 mg/L. The fluorogenic detection were carried out in PBS buffer with pH = 7.4. [**TC426**] = 10 μM, λ_{ex} = 480 nm, I_0 equals the intensity of [HSA] = 0 mg/L.

Selectivity and Interference Study

Due to the chemical complexity of human urine, that includes a wide pH value (5.5-7.0) and various components (urea, uric acid, creatinine, inorganic salts, etc.), practical application of **TC426** in urine should evaluate the environmental interferences first. Here, we evaluated the effect of pH values on the sensing process of **TC426** towards HSA. As shown in **Figure 3A**, in the absence of HSA, no fluorescence can be detected. In contrast, after addition of 1000 mg/L HSA, the fluorescence intensity of **TC426** increased markedly and remained stable in the pH range of 5.0-7.0. Even though the measured fluorescence intensity is slightly higher under extreme conditions (pH = 4.0 or 8.0), this impact may be reduced through diluting urine samples with PBS buffer. Based on the results, it can be concluded that probe **TC426** is able to detect HSA in a wide range of pH values.

The specificity of probe **TC426** toward HSA was then compared to a variety of ions, commonly found in biological fluids. As shown in **Figure 3B**, no fluorescence enhancement was observed after the addition of those ions. Proteins with different isoelectric points (ranging from 1 to 10) were then selected for study, including pepsin, BSA, ubiquitin, papain, and trypsin. Apart from a minor response from BSA, whose structure is similar to HSA, none of the other proteins were observed to elicit a large fluorescence intensity enhancement in **TC426**. Fluorescence responses of **TC426** towards amino acid glutathione (GSH) and nucleic acid RNA were also examined and show minimal fluorescence variations under the same test conditions (**Figure 3C**). These results demonstrate the excellent selectivity probe **TC426** has for HSA over other biomolecules or ions and can be applied in complex biological environments.

Since probe **TC426** can be potentially applied in urinalysis, we further evaluated the influence of other major components in human urine on this detection. Some common organic components in urine include urea, uric acid, creatinine, and glucose and were selected for testing. The experimental results shown in **Figure 3D** suggested that these urine interferents have limited influence on the fluorescence emission of **TC426** in the presence or absence of HSA. Additionally, we compared the influence of these components on **TPE-4TA** and **BSPOTPE**. It can be seen that the fluorescence responses of both **TC426** and **TPE-4TA** are more stable than that of probe **BSPOTPE** in the presence of interferents. In brief, the novel fluorescent probe **TC426** shows great potential in detecting HSA in real urine samples.

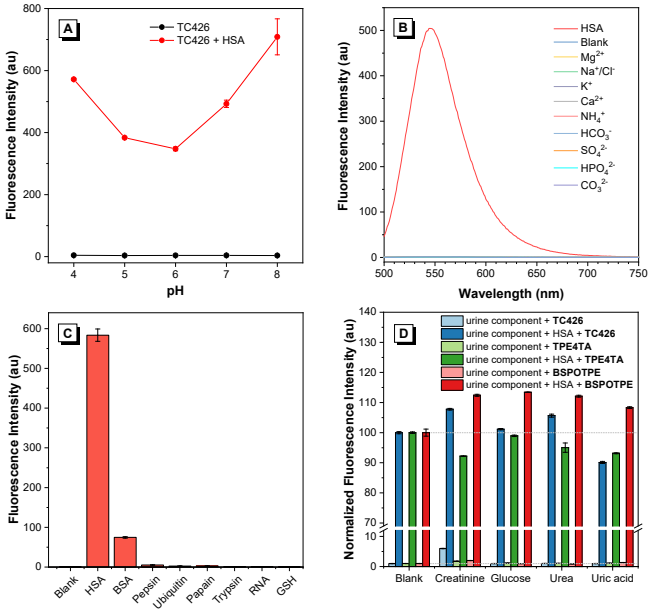

Figure 3. Study of the HSA sensing performance of **TC426** at different conditions. (A) Fluorescence intensity variation of probe **TC426** and HSA-**TC426** mixture at 550 nm in a pH gradient. [HSA] = 1000 mg/L. (B) Fluorescence spectra of **TC426** in the presence of various common cations and anions in PBS buffer (pH = 7.4). [HSA] = 1000 mg/L, [ions] = 10 mM. (C) Fluorescence response of probe **TC426** toward biomolecules in PBS buffer. [Biomolecules] = 1 mg/mL. (D) Interference of common components in urine on the fluorescence intensity of HSA probes **TC426**, **TPE-4TA** and **BSPOTPE** in the presence/absence of HSA in PBS buffer. [HSA] = 1000 mg/L, [urine component] = 10 mg/mL. For all the measurements, [**TC426**] = 10 μM, λ_{ex} = 480 nm.

Sensing mechanism

Since probe **TC426** shows excellent performance in HSA detection, we further studied its sensing mechanism. Firstly, we performed the Job plot analysis to study the binding stoichiometry between **TC426** and HSA. As shown in **Figure 4A**, the fluorescence intensity reached the maxima when the ratio of **TC426** was among 0.3 to 0.4, which suggested that the binding ratio between **TC426** and HSA is approx. 1:2. This observation suggested **TC426** interacts with HSA as a monomeric species rather than as aggregates, which is in accord with the emission peak observed at ~550 nm (monomer). Secondly, we investigated the relationship between fluorescence intensity of **TC426** and tertiary structure of HSA. As we know, HSA has two major drug binding sites, site I and site II in subdomains IIA and IIIA, respectively. Most of the reported HSA probes interact with these drug binding sites mainly through hydrogen bonding, hydrophobic interaction, or electrostatic effects. Some literatures have reported strategies for studying HSA sensing mechanism,

including using ligand displacement strategy, protein denaturation, isothermal titration calorimetry, and molecular docking calculation.[16] Here we applied the protein denaturation strategy using urea denaturant which can break the stability of internal non-covalent bonds and destroy the tertiary structure of HSA under high concentrations (4-8 M). We carried out the fluorescence assay with urea concentration ranging from 0-10 M. As shown in **Figure 4B**, the whole process of HSA denaturation is a three-step process. When the concentration of urea is between 0-2 M, limited protein denaturation occurred, and albumin is still in its native state. The increase of fluorescence intensity maybe due to the swelling effect of HSA, which facilitates the dye molecule to get into the interior domain.[12a] With the increase of urea up to 2-4 M, HSA undergoes partial unfolding to reach an intermediate state, which provides a hydrophobic environment for the bound dye. As indicated in Table S1, the lower the solvent polarity, the higher the quantum yield. Therefore, at this stage, the fluorescence intensity further increases, mainly contributed from the hydrophobic effect. Afterwards, the continuous denaturation of albumin by higher concentration of urea, causing the loss of secondary structure, is manifested in the continuous decrease of fluorescence intensity, and finally reaches at a completely denatured state. This protein denaturation experiment proved that the sensing process is closely related to the tertiary and secondary structure of HSA. Additionally, since the QY of **TC426** shows obvious polarity dependence, it can be concluded that the fluorescence enhancement during HSA detection is caused by the movement of probe **TC426** from polar aqueous environment to the low polar cavities of HSA (**Figure 4C**). As such, **TC426** acts as an environmentally sensitive probe for HSA detection.

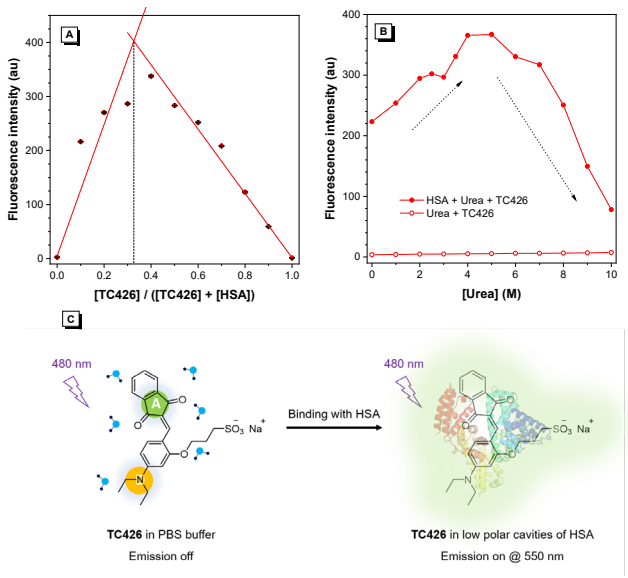

Figure 4. (A) Job plot for determination of the binding stoichiometry of **TC426** and HAS. The total concentration of **TC426** and HSA was kept constant as 10 μM in PBS buffer. (B) Variation in the fluorescence intensity of **TC426** at 550 nm with concentration of urea in the presence or absence of HSA. [**TC426**] = 10 μM, [HSA] = 100 mg/L, λ_{ex} = 480 nm. (C) Schematic of the working mechanism of probe **TC426** in HSA detection.

Detection of HSA in real human urine

Due to its excellent performance in detecting HSA from PBS buffer, we further studied the feasibility of applying **TC426** in real urine environment. Firstly, fluorescence titration in spiked human urine samples obtained from three healthy individuals was conducted to give an adjusted calibration curve which should be more suitable for practical applications (**Figure S11**). HSA spiked urine samples were diluted 10 times using PBS buffer (pH = 7.4) to eliminate the effect of pH values and autofluorescence from real urine. As shown in **Figure 5**, a good linear correlation between fluorescence intensity of **TC426** and HSA concentration can be observed in the range of 0-200 mg/L. In order to simulate the application of probe **TC426** to HSA detection in real scenarios, real human urine samples collected randomly from another two healthy people were spiked with certain amounts of HSA for recovery study. Since the diagnosis of microalbuminuria has significant importance in the early detection of CKD, the calculated concentrations of these urine samples are located in the microalbuminuria range, which are 50, 125, and 175 mg/L, respectively. With the newly established fluorescence assay and adjusted calibration curve, the recovered HSA concentrations were measured and presented in **Table 1**. Satisfactory recovery rates in the range of 81.3-129.9% with standard deviations ranging from 1.5 to 10.7% were obtained. This indicates that probe **TC426** can be applied to the detection of HSA in real urine samples.

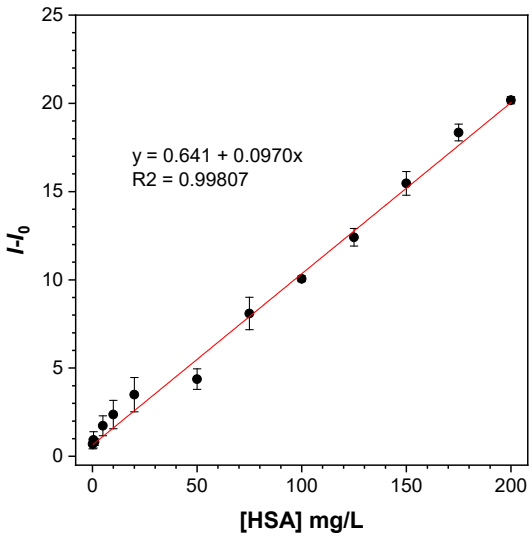

Figure 5. Plot of HSA concentration in real urine from health person versus the corresponding fluorescence intensity increase at 550 nm by the fluorescent assay using **TC426** (Y-axis). I_0 equals to the fluorescence intensity at 550 nm of real urine without adding HSA. Three repeats for each concentration were conducted in urine from different healthy individuals. [**TC426**] = 10 μM, λ_{ex} = 480 nm.

Table 1. Result of recovery study on the novel fluorescence assay using HSA spiked real urine samples.

Spiked Conc. (mg/L)	Urine from volunteer 1		**Urine from volunteer 2**	
	Recovered Conc. ± SD (mg/L)	**Recovery Rate (%)**	**Recovered Conc. ± SD (mg/L)**	**Recovery Rate (%)**
50.0	40.7 ± 1.8	81.3 ± 3.5	48.8 ± 5.3	97.7 ± 10.7
125.0	119.7 ± 2.1	95.8 ± 1.7	162.4 ± 2.6	129.9 ± 2.1
175.0	204.7 ± 5.3	117.0 ± 3.0	209.2 ± 2.7	119.5 ± 1.5

Conclusion

In summary, we designed a novel 'turn-on' fluorescent probe, **TC426** for the quantitative detection of HSA. This probe can be synthesized simply via a two-step reaction, and AIE characteristics were comprehensively investigated. Afterwards, probe **TC426** was applied in the detection of HSA. The result of fluorescence titration shows a wide linear dynamic range (0-1000 mg/L) and a low detection limit 0.253 mg/L of probe **TC426**. Moreover, experiments proved that the sensing mechanism is through the environmental polarity response of **TC426** in the tertiary structure of HSA. Before application in real urine samples, effect of pH value and common interferents from body fluids were evaluated, manifesting its high selectivity towards HSA and good stability in complex environments. Finally, the detection of HSA in real human urine by probe **TC426** was validated, resulting in a satisfactory accuracy and recovery rate. Therefore, probe **TC426** shows the promise to be further developed into an effective clinical method for quantitative detection of HSA in human urine.

Experimental Section

Materials and Instruments. 1,3-Propanesultone, inorganic salts (NaCl, KCl, $MgCl_2$, $CaCl_2$, NH_4Cl, Na_2CO_3, $NaHCO_3$, Na_2SO_4, and Na_2HPO_4), proteins (HSA, BSA, pepsin, ubiquitin, papain, and trypsin), RNA, GSH, PBS tablets, glycerol, uric acid, creatinine, glucose, and chromatographically pure solvents (DMSO, toluene, chloroform, etc.) were all purchased from Sigma-Aldrich. Hydrochloric acid and sodium hydroxide were obtained from Chem-supply. Urea was obtained from Chem-supply. 4-(Diethylamino)salicylaldehyde was obtained from AK Scientific. 1,3-Indanedione was obtained from Alfa Aesar. Probes **BSPOTPE** and **TPE-4TA** were synthesized according to previously publications [11, 13]. ^{1}H (400 MHz) & ^{13}C NMR (100 MHz) spectra were acquired on Agilent MR400 or Agilent DD2 instrument. The chemical shift data for each signal are given as *δ*. High-resolution mass spectra were acquired using a Thermo Scientific Q Exactive Plus Orbitrap LC-MS/MS instrument. Absorbance and fluorescence spectra were obtained on a Cary 300 UV-Vis spectrometer and Cary Eclipse fluorimeter (Agilent Technologies Inc., USA), respectively. Particle size distributions were measured in triplicate on Zetasizer Nano ZEN3600 (Malvern Instruments Ltd, Malvern, WR14 1XZ, United Kingdom). pH values were adjusted using HANNA HI208 pH meter. Data were plotted using Origin 2018 (OriginLab Corp., USA).

Synthetic Procedures.
Probe **TPE-4TA**[17] and **BSPOTPE**[18] were synthesized according to previous publications and supplied by AIEgen Biotech Co., Ltd, China. The synthetic route to **TC426** was shown in **Scheme 1** and detailed synthesis procedures were shown as following.

Synthesis of 2-(4-(diethylamino)-2-hydroxybenzylidene)-1H-indene-1,3(2H)-dione (**2**). 4-(Diethylamino)salicylaldehyde (1, 9.66 g, 50 mmol) was added to 1,3-indanedione (6.58 g, 45 mmol). A mixture of ethanol (100 mL) and water (50 mL) was then added. The reaction mixture was then stirred and heated at 75 °C for 3 h. Upon completion of the reaction, the reaction mixture was cooled to room temperature and 100 mL of water was added. The precipitates were filtered and washed with an ethanol: water mixture (1:1 x 1 and 1:5 x 2) to give the product as a dark red solid in 70% yield (11.2 g). ^{1}H NMR (400 MHz, DMSO-d_6) δ 10.71 (s, 1H), 9.21 (d, *J* = 9.4 Hz, 1H), 8.19 (s, 1H), 7.77 (s, 4H), 6.43 (d, *J* = 9.4 Hz, 1H), 6.18 (s, 1H), 3.76 – 3.14 (m, 4H), 1.15 (t, *J* = 7.0 Hz, 6H). ^{13}C NMR (101 MHz, DMSO-d_6) δ 191.54, 189.71, 163.94, 155.39, 141.74, 140.01, 139.37, 136.69, 134.86, 134.59, 122.18, 122.11, 118.84, 111.20, 105.81, 96.17, 44.91, 13.12. HRMS (ESI+): *m*/*z*. 322.14319 [$C_{20}H_{20}NO_3$ $(M+H)^+$, calcd 322.14322].

Synthesis of sodium 3-(5-(diethylamino)-2-((1,3-dioxo-1,3-dihydro-2H-inden-2-ylidene)methyl)phenoxy)propane-1-sulfonate (**TC426**). Intermediate compound **2** (500 mg, 1.56 mmol) was added with NaOH (74.9 mg, 1.87 mmol) and taken up in ethanol (20 mL) and stirred at room temperature for 30 min. 1,3-propanesultone (419 mg, 3.43 mmol) was taken up in ethanol (10 mL), slowly added to the reaction mixture before heating at 75 °C for 12 h. Upon completion of the reaction, the reaction mixture was cooled to room temperature and poured into ethanol. The precipitate was then filtered and washed with ethanol (x3) to obtain the pure product as a red solid in 36% yield (258 mg). ^{1}H NMR (400 MHz, DMSO-d_6) δ 9.27 (d, *J* = 9.4 Hz, 1H), 8.20 (s, 1H), 7.78 (s, 4H), 7.58 (d, *J* = 5.6 Hz, 1H), 6.50 (d, *J* = 10.4 Hz, 1H), 6.24 (s, 1H), 4.28 (t, *J* = 6.6 Hz, 2H), 3.54 (q, *J* = 6.8 Hz, 4H), 2.60 (t, *J* = 7.1 Hz, 2H), 2.26 – 1.75 (m, 2H), 1.16 (t, *J* = 6.9 Hz, 6H). ^{13}C NMR (100 MHz, DMSO-d_6) δ 191.34, 189.61, 163.61, 155.57, 141.76, 139.56, 139.39, 136.99, 134.91, 134.66, 132.92, 122.25, 122.17, 120.80, 119.42, 111.69, 105.65, 93.96, 67.80, 48.07, 25.48, 13.16. HRMS (ESI-): *m*/*z*. 442.13155 [$C_{23}H_{24}NO_6S$ $(M-Na)^-$, calcd 442.13298].

Experimental operations of HSA detection:
Preparation of dye solutions:
TC426 was dissolved in dimethyl-sulfoxide (DMSO) solution, the stock solution was made to 10 mM and kept at -20 °C in the dark for long term storage. Moreover, the recommended working solution of **TC426** was prepared daily by suitable dilution of the stock solution with PBS buffer to 10 μM. **TPE-4TA** and **BSPOTPE** stock solution (10 mM) was prepared in PBS buffer and can be stored at 4 °C in the dark for further use.

Preparation of HSA samples in PBS buffer:
HSA stock solution with a concentration of 1000 mg/L was first prepared in PBS buffer and stored under 0-4 °C. The stock solution was diluted stepwise to our desired concentrations including: 0.1, 0.5, 1, 5, 10, 20, 50, 75, 100, 125, 150, 175, 200, 500, 700 mg/L. Moreover, each concentration must have three parallel samples for three repeated fluorescence measurement.

*Preparation of HSA-**TC426** mixtures in PBS buffer for fluorescence measurement:*
Pipette 1.998 mL of the above prepared HSA samples and 0.002 mL **TC426** stock solution to an Eppendorf tube. Shake each mixture with vortex shaker violently for 10s to obtain HSA-**TC426** samples with [TC**426**] = 10 μM and [HSA] = 0.1, 0.5, 1, 5, 10, 20,

50, 75, 100, 125, 150, 175, 200, 500, 700, and 1000 mg/L. Finally, the HSA-**TC426** samples were transferred into a quartz cuvette for fluorescence measurement.

Study on pH influence:
One PBS tablet was dissolved in 180 mL DDI water to afford the PBS buffer with pH value around 7.4. Afterward, 1 M hydrochloric acid and sodium hydroxide aqueous solutions were used to adjust the pH value to 4, 5, 6, 7 and 8, respectively. Finally, add DDI water until the total volume of each solution reach 200mL. For the study of pH influence, HSA solid powder was dissolved in PBS buffer with different pH values to give a final HSA concentration of 1000 mg/L. Then stock solution of **TC426** was added, mixed using vortex shaker, incubated for 20 min, and measured using fluorescence spectrometer. The fluorescence of PBS buffers with only probe **TC426** added were also measured for comparison.

Study on selectivity:
Certain amount of salt powders (sodium chloride, potassium chloride, magnesium chloride, calcium chloride, ammonium chloride, sodium bicarbonate, sodium sulfate, disodium hydrogen phosphate and sodium carbonate) were weighed and dissolved in the PBS buffer (pH 7.4), respectively, to give the ionic solutions with concentrations of 10 mM. Afterwards, 1.998 mL ion solutions, as well as PBS buffer and HSA solution (1000 mg/L), were added with 0.002mL **TC426** stock solution to afford different samples for fluorescence measurement. Similarly, eight common biomolecules which are BSA, Pepsin, Ubiquitin, Papain, Trypsin, RNA, GSH and HSA were selected to explore the probe protein response at 1 mg/mL in PBS buffer. The fluorescence intensity of these samples was measured at room temperature according to the previous operation procedures.

Study on interference:
Common urine components including uric acid, urea, creatinine and glucose, were dissolved in PBS buffer (pH = 7.4) at 10 mg/mL. Notably, due to the limited water solubility of uric acid, the concentration of uric acid applied is about 0.3 mg/mL. The concentration of HSA is 1000 mg/L. The concentration of bioprobes **TC426**, **TPE-4TA** and **BSPOTPE** after mixing with interferents were all 10 μM. During the whole measurement process, the three probe stock solutions were added separately into five urine components samples (v/v 1:999) to mix evenly. The excitation/emission maxima wavelength of **TC426**, **TPE-4TA** and **BSPOTPE** are 480/550 nm, 360/490 nm and 350/470 nm, respectively.

Mechanism study:
Firstly, lyophilized powder of HSA was dissolved in PBS buffer (pH 7.4) with a concentration of 10 mg/L. Then, different amounts of urea were added to the as-prepared HSA solution to prepare samples with urea concentration ranging from 0 to 10 M. Afterward, 0.002 mL probe **TC426** stock solution was added to each HSA/urea solutions and incubated for 1 hour to ensure that the protein denaturation was fully occurred. At last, fluorescence spectra were recorded using a fluorescence spectrophotometer.

HSA detection in spiked human urine samples:
Human urine samples were collected from three healthy volunteers (one female and two males) from Flinders University and tested following the guide from the Southern Adelaide Clinical Human Research Ethics Committee, Australia. First of all, based on the previously standard curve in PBS buffer, HSA samples with concentrations of 0, 0.1, 0.5, 1, 5, 10, 20, 50, 75, 100, 125, 150, 175 and 200 mg/L were similarly prepared in the urine samples of subjects and diluted ten times with PBS buffer. After that, 0.002 mL of **TC426** stock solution was mixed with 1.998 mL of the (diluted) urine sample and was fully mixed by vortex shaker for 10 seconds. The mixture was transferred to a cuvette and fluorescence spectra were recorded using a Cary Eclipse Fluorescence Spectrophotometer.

Recovery study:
HSA solutions with concentrations of 0, 50, 125, and 175 mg/L were prepared respectively in urine samples collected from two healthy male volunteers (different individuals from the above methioned male volunteers) from Flinders University. According to the obtained master curve in real human urine, the increase of fluorescence intensity measured from these samples were substituted into the master curve to calculate the recovered concentrations and recovery rates.

Acknowledgements

We acknowledge the Australia-China Science and Research Fund, Joint Research Centre on Personal Health Technologies for support.

Keywords: human serum albumin • fluorescence probe • aggregation-induced emission • turn-on response • urinalysis

[1] J. Nicholson, M. Wolmarans, G. Park, *British journal of anaesthesia* **2000**, *85*, 599-610.

[2] a) S. Prakash, *J Appl Biotechnol Bioeng* **2017**, *3*, 00057; b) G. Fanali, A. di Masi, V. Trezza, M. Marino, M. Fasano, P. Ascenzi, *Mol Aspects Med* **2012**, *33*, 209-290.

[3] D. G. Levitt, M. D. Levitt, *International journal of general medicine* **2016**, *9*, 229.

[4] a) P. Lee, X. Wu, *Current pharmaceutical design* **2015**, *21*, 1862-1865; b) F. Yang, Y. Zhang, H. Liang, *Int J Mol Sci* **2014**, *15*, 3580-3595; c) J. Tong, T. Hu, A. Qin, J. Z. Sun, B. Z. Tang, *Faraday Discuss* **2017**, *196*, 285-303; d) U. Kragh-Hansen, *Biochim Biophys Acta* **2013**, *1830*, 5535-5544.

[5] a) M. Anraku, K. Yamasaki, T. Maruyama, U. Kragh-Hansen, M. Otagiri, *Pharmaceutical research* **2001**, *18*, 632-639; b) V. M. Rosenoer, M. Oratz, M. A. Rothschild, *Albumin: Structure, function and uses*, Elsevier, **2014**; c) B. Yao, M.-C. Giel, Y. Hong, *Materials Chemistry Frontiers* **2021**; d) X. Zhang, B. Yao, Q. Hu, Y. Hong, A. Wallace, K. Reynolds, C. Ramsey, A. Maeder, R. Reed, Y. Tang, *Materials Chemistry Frontiers* **2020**, *4*, 2548-2570.

[6] J.-F. Xu, Y.-S. Yang, A.-Q. Jiang, H.-L. Zhu, *Critical Reviews in Analytical Chemistry* **2020**, 1-21.

[7] a) H. Martin, *The Clinical Biochemist Reviews* **2011**, *32*, 97; b) W. D. Comper, T. M. Osicka, G. Jerums, *Am J Kidney Dis* **2003**, *41*, 336-342.

[8] a) O. H. Lowry, N. J. Rosebrough, A. L. Farr, R. J. Randall, *J. Biol. Chem.* **1951**, *193*, 265-275; b) J. H. Eckfeldt, M. J. Kershaw, I. I. Dahl, *Clin. Chem.* **1984**, *30*, 443-446; c) ; d) G. F. Grauer, *Top Companion Anim Med* **2011**, *26*, 121-127.

[9] D. Y. Gaitonde, D. L. Cook, I. M. Rivera, *American family physician* **2017**, *96*, 776-783.

[10] a) Y. Hong, J. W. Lam, B. Z. Tang, *Chemical Society Reviews* **2011**, *40*, 5361-5388; b) Y. Hong, J. W. Lam, B. Z. Tang, *Chemical communications* **2009**, 4332-4353; c) R. T. Kwok, C. W. Leung, J. W. Lam, B. Z. Tang, *Chemical Society Reviews* **2015**, *44*, 4228-4238; d) H. Kobayashi, M. Ogawa, R. Alford, P. L. Choyke, Y. Urano, *Chemical*

reviews **2010**, *110*, 2620-2640; e) J. Mei, N. L. Leung, R. T. Kwok, J. W. Lam, B. Z. Tang, *Chem Rev* **2015**, *115*, 11718-11940; f) J. Liang, B. Z. Tang, B. Liu, *Chem Soc Rev* **2015**, *44*, 2798-2811; g) X. Gu, R. T. K. Kwok, J. W. Y. Lam, B. Z. Tang, *Biomaterials* **2017**, *146*, 115-135; h) Y. Hong, L. Meng, S. Chen, C. W. T. Leung, L.-T. Da, M. Faisal, D.-A. Silva, J. Liu, J. W. Y. Lam, X. Huang, *Journal of the American Chemical Society* **2012**, *134*, 1680-1689.

[11] Y. Hong, C. Feng, Y. Yu, J. Liu, J. W. Y. Lam, K. Q. Luo, B. Z. Tang, *Analytical chemistry* **2010**, *82*, 7035-7043.

[12] a) W. Li, D. Chen, H. Wang, S. Luo, L. Dong, Y. Zhang, J. Shi, B. Tong, Y. Dong, *ACS Appl Mater Interfaces* **2015**, *7*, 26094-26100; b) Y. Yu, Y. Huang, F. Hu, Y. Jin, G. Zhang, D. Zhang, R. Zhao, *Anal Chem* **2016**, *88*, 6374-6381; c) J. Li, J. Wu, F. Cui, X. Zhao, Y. Li, Y. Lin, Y. Li, J. Hu, Y. Ju, *Sensors and Actuators B: Chemical* **2017**, *243*, 831-837; d) L. Gao, X. Lin, X. Chen, *Talanta* **2020**, *212*, 120763; e) Z. Luo, T. Lv, K. Zhu, Y. Li, L. Wang, J. J. Gooding, G. Liu, B. Liu, *Angew Chem Int Ed Engl* **2020**, *59*, 3131-3136; f) S. Halder, S. Samanta, G. Das, *Analyst* **2019**, *144*, 2696-2703.

[13] Y. Tu, Y. Yu, Z. Zhou, S. Xie, B. Yao, S. Guan, B. Situ, Y. Liu, R. T. Kwok, J. W. Lam, *ACS applied materials & interfaces* **2019**, *11*, 29619-29629.

[14] S. Sasaki, G. P. C. Drummen, G.-i. Konishi, *Journal of Materials Chemistry C* **2016**, *4*, 2731-2743.

[15] a) M. T. James, B. R. Hemmelgarn, M. Tonelli, *The Lancet* **2010**, *375*, 1296-1309; b) A. S. Narva, *Scandinavian Journal of Clinical and Laboratory Investigation* **2008**, *68*, 12-15.

[16] a) Z. Luo, B. Liu, K. Zhu, Y. Huang, C. Pan, B. Wang, L. Wang, *Dyes and Pigments* **2018**, *152*, 60-66; b) S. Muzammil, Y. Kumar, S. Tayyab, *Proteins: Structure, Function, and Bioinformatics* **2000**, *40*, 29-38; c) H. Li, Q. Yao, J. Fan, J. Du, J. Wang, X. Peng, *Dyes and Pigments* **2016**, *133*, 79-85; d) Y. Huang, T. Lv, T. Qin, Z. Xu, L. Wang, B. Liu, *Chem Commun (Camb)* **2020**, *56*, 11094-11097; e) K. Zhu, T. Lv, T. Qin, Y. Huang, L. Wang, B. Liu, *Chem Commun (Camb)* **2019**, *55*, 13983-13986.

[17] S. Xie, A. Y. H. Wong, R. T. K. Kwok, Y. Li, H. Su, J. W. Y. Lam, S. Chen, B. Z. Tang, *Angew Chem Int Ed Engl* **2018**, *57*, 5750-5753.